Conical refraction lasing in a Nd: YVO4 laser with a conerefringent KGW element

R. Akbari, C. Howlader, K. A. Fedorova, G. S. Sokolovskii, E. U. Rafailov, et al.

R. Akbari, C. Howlader, K. A. Fedorova, G. S. Sokolovskii, E. U. Rafailov, A. Major, "Conical refraction lasing in a Nd:YVO4 laser with a conerefringent KGW element," Proc. SPIE 10904, Laser Resonators, Microresonators, and Beam Control XXI, 109041Z (4 March 2019); doi: 10.1117/12.2508960

SPIE.

Event: SPIE LASE, 2019, San Francisco, California, United States

Conical refraction lasing in a Nd:YVO_4 laser with a conerefringent KGW element

R. Akbari[1], C. Howlader[1], K.A. Fedorova[2], G.S. Sokolovskii[3,4], E.U. Rafailov[5,6], and A. Major[1]
[1] Department of Electrical and Computer Engineering, University of Manitoba, Winnipeg, R3T 5V6, Canada
[2] Department of Physics, Philipps-Universität Marburg, Marburg, 35032, Germany
[3] Ioffe Institute, St. Petersburg, 194021, Russia
[4] Saint Petersburg Electrotechnical University (LETI), St. Petersburg, 197022, Russia
[5] School of Engineering & Applied Science, Aston University, Birmingham, B4 7ET, UK
[6] Saratov State University, Astrakhanskaya Str. 83, Saratov 410012, Russia

Keywords: Conical refraction, solid-state laser, diode-pumped laser, Nd-doped laser crystals

ABSTRACT

A conical refraction (CR) laser based on a separate gain medium (Nd:YVO_4) and an intracavity CR element (KGW) was demonstrated. The decoupling of the gain and CR media enabled the laser to produce a well-behaved CR laser beam with excellent quality, while reducing the complexity of the pumping scheme. The proposed laser setup has the potential for power scaling using the efficient diode pumping approach and the properties of the generated CR beam are independent from the laser gain medium.

1. INTRODUCTION

The well-known conical refraction (CR) phenomenon has attracted attention in recent years due to its fundamental properties and practical applications in, e.g., optical trapping, microscopy and optical communications [1]. In principle, a biaxial crystal cut along its optical axis transforms a beam with Gaussian intensity distribution into a pair of bright concentric rings separated by a dark Poggendorff ring in the focal (Lloyd) plane [1]. Another unique characteristic of the conically refracted beam is that any two diametrical points on the ring have orthogonal polarizations. In addition, the CR beam evolves symmetrically about the Lloyd plane into a bright central (Raman) spot in the far field. The generation of CR beams using an external laser beam (also called "passive CR") have been demonstrated and studied in numerous works [1-8]. However, "active" CR beams delivered directly from the laser oscillators have only been recently demonstrated where the laser medium also acts as a CR element [9-14]. Due to the complex relationship between the classical effect of CR, anisotropic laser gain as well as the resonant conditions of the optical cavity, the properties of "active" laser CR are still not well known. For example, in some cases a Gaussian beam was produced after the plane output mirror, while in the other experiments the output beam had a crescent-like shape without a clear double-ring pattern (i.e. without a dark Poggendorff ring).

In this work we demonstrated a simple solution to reduce the complexity of the "active" CR by decoupling the gain and CR media or conerefringent element (CRE). The advantages of the proposed laser are that an optimal laser gain and CR conditions can be achieved more independently and the laser properties are not limited by the properties of the CR element. In addition, a separate laser gain medium allows for power scaling. Our laser setup used a Nd:YVO_4 crystal as the gain medium and KGW crystal as the intracavity CR element. The laser produced images of the CR laser beams of unprecedented quality with output power up to 220 mW with 500 mW of pump power. In experiments one of the main CR laser beam forming conditions was identified and experimentally confirmed.

Laser Resonators, Microresonators, and Beam Control XXI, edited by Alexis V. Kudryashov, Alan H. Paxton, Vladimir S. Ilchenko, Proc. of SPIE Vol. 10904, 109041Z · © 2019 SPIE
CCC code: 0277-786X/19/$18 · doi: 10.1117/12.2508960

2. EXPERIMENTAL SETUP

The laser used a 3 mm-long a-cut 1.1 at.% Nd:YVO_4 laser crystal as the gain medium in a five-mirror laser cavity, as shown in figure 1. The highly polarized laser emission and efficient laser operation in the continuous-wave (CW) and pulsed regimes are characteristics of this vanadate crystal [15-19]. The crystal had anti-reflective (AR) coatings for the pump wavelength (~808 nm) and laser wavelength (1064 nm) on both surfaces. The laser crystal was pumped by a home-built Ti:sapphire laser with oscillating wavelength at 808.8 nm which was tuned by means of a 0.5 mm birefringent filter (see figure 1). This wavelength corresponds to the maximum absorption of the Nd:YVO_4 crystal. The Ti:sapphire laser could deliver up to 500 mW of output power and the beam was focused into a spot size of around 35 μm in the Nd:YVO_4 crystal. The R3 mirror provided the required focusing of the laser mode into the CRE (see figure 1). The CRE was an 18 mm-long AR-coated KGW crystal ($KGd(WO_4)_2$) cut along its optical axis. The KGW crystal is a popular choice for the active/passive CR experiments [9,11–14,20–23]. Strong anisotropy of optical and physical properties as well as high optical quality are features of the KGW crystal which make it a suitable host for rare-earth metal ion based lasers in the CW and pulsed regimes [24-33].

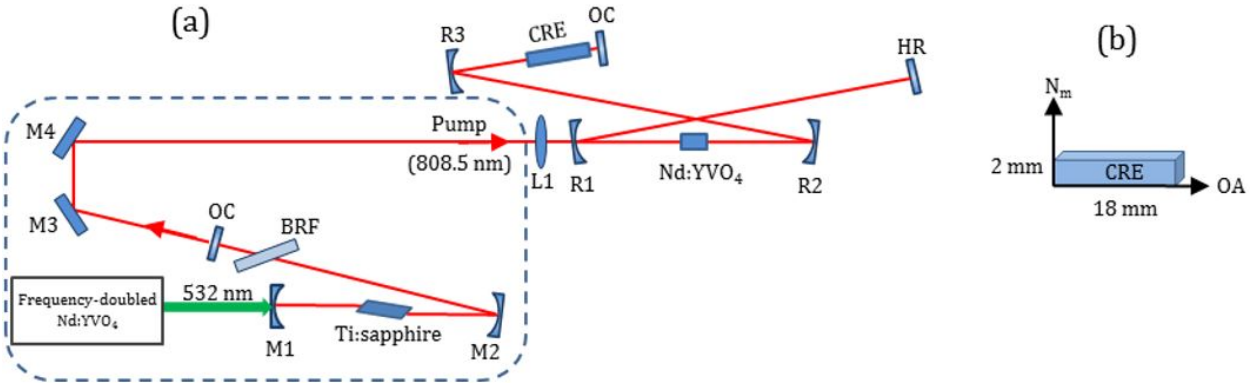

Figure 1. (a) Schematic of the laser cavity. The output of the Ti:sapphire laser was used as the pump for the Nd:YVO_4 laser. For CR Nd:YVO_4 laser cavity R1 = R2 = −100 mm, R3 = −150 mm. BRF: birefringent filter, OC: output coupler, HR: highly reflective mirror, CRE: conerefringent element. (b) Schematic of the CRE (KGW crystal), OA: optical axis.

3. RESULTS AND DISCUSSION

The Nd:YVO_4 laser was initially operated without the CRE in the cavity and generated a typical beam with Gaussian intensity distribution and horizontal polarization at 1064.35 nm. By using a 5% output coupling, the laser delivered more than 300 mW of output power for 500 mW of pump power. In order to operate the laser in the CR regime, the KGW crystal (i.e. CRE) was inserted in the R3-OC arm of the cavity with its N_m-axis oriented horizontally (see figure 1). The R3-OC arm of the cavity was correspondingly adjusted (i.e. increased) in order to retain the stability of the laser. The output of the CR laser (i.e. a laser with an intracavity CRE) was monitored using an imaging lens (f=60 mm) and a CCD camera. For large misalignment of the CRE optical axis (OA) and cavity mode axis, a double refraction of the laser output with two distinct bright spots was observed. By further adjustment of the CRE, the laser beam approached the ring-shaped pattern with increased output power. Fine alignment of the CRE was required to bring the OA of the CRE into a parallel position with the cavity axis in order to observe a fully resolved CR pattern with a dark Poggendorff ring (see figure 2 (a)). The position of the image plane (i.e. Lloyd image plane) was estimated to be around 3-5 mm outside of the output coupler. For this orientation of the CRE (i.e. horizontal N_m-axis) the node of the CR pattern was at the bottom of the beam. In addition, the generated CR laser beam exhibited evolution pattern along its propagation axis similar to the well-known free-space CR beam, i.e. from the Lloyd image plane towards the Raman spot, as shown in figure 2(b)-(e). In this regime of operation, the CR laser

could deliver up to 220 mW of output power for maximum pump power of 500 mW. To further confirm the CR nature of the obtained radiation, the polarization distribution along the CR beam ring pattern was determined by using a rotating polarizer. In this case the polarization rejected by the polarizer appeared as an additional dark spot on the image of beam intensity profile (see figure 2 (f)-(i)). As can be seen, the diametrically opposite points along the beam possessed orthogonal polarization states.

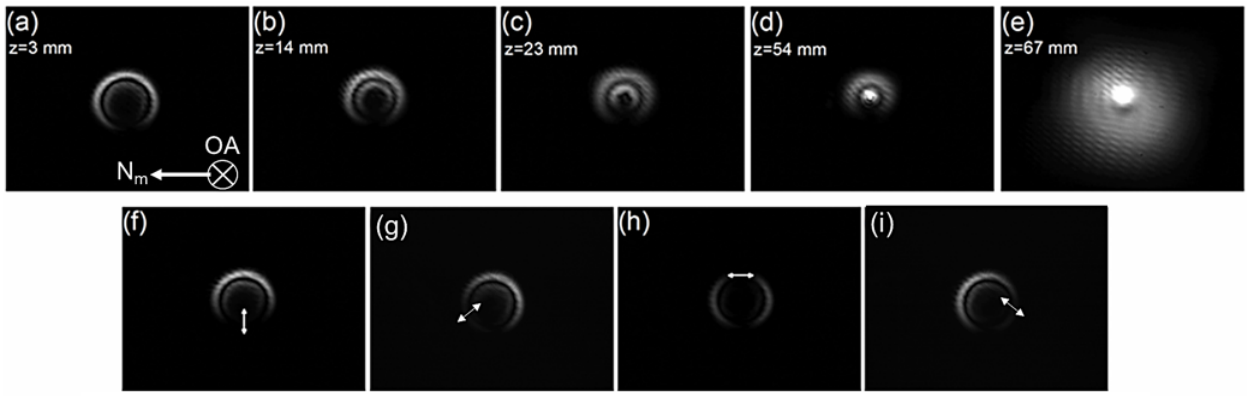

Figure 2. The CR laser beam at the Lloyd image plane and its free-space evolution for the CRE with horizontal orientation of the N_m-axis (a)-(e). The local polarization states along the CR beam were determined by polarizer and are marked by arrows in (f)-(i). The numbers in the first row show the calculated positions of the image planes from the outer surface of the output coupler. The far-field beam in (e) was imaged without an imaging lens.

The generation of the CR laser beam was also investigated for orthogonal orientation of the CRE (i.e. for vertical N_m-axis). In this case the node of the CR beam was positioned on the side of the CR ring and the beam exhibited similar evolution pattern along its propagation axis (see figure 3 (a)-(e)). In addition, the polarization state distribution along the beam was rotated by 90 degrees (see figure 3 (f)-(i)).

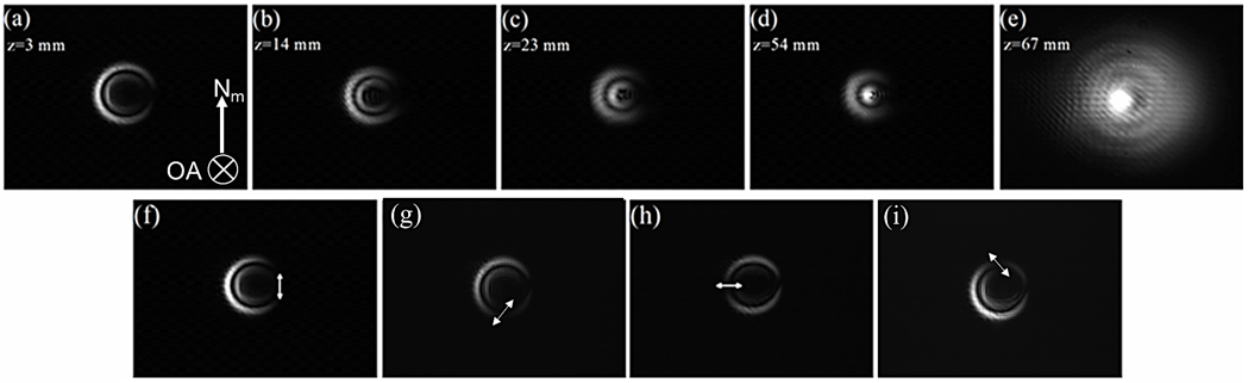

Figure 3. The CR laser beam at the Lloyd image plane and its free-space evolution for the CRE with vertical orientation of the N_m-axis (a)-(e). The polarization states along the CR beam were determined by polarizer and are marked by arrows in (f)-(i). The numbers in show the calculated positions of the image planes from the outer surface of the output coupler. The far-field beam in (e) was imaged without an imaging lens.

In order to compare the performance of the CR laser with an equivalent Gaussian laser (i.e. a laser without an intracavity CRE), a 20 mm-long AR-coated N_g-cut (non-CR) KGW crystal was inserted instead of the CRE in the cavity. The laser produced an output beam with intensity distribution of a fundamental Gaussian mode. The laser delivered the maximum output power of 287 mW for 500 mW of incident pump power with the slope efficiency of 58%, while the CR laser could deliver the maximum output power of 220 mW with the slope efficiency of 44%. The

Gaussian laser without the additional KGW crystal (i.e. CR or non-CR KGW crystals) generated the maximum output power of 307 mW with the slope efficiency of 63%. The performance of these lasers is compared in figure 4.

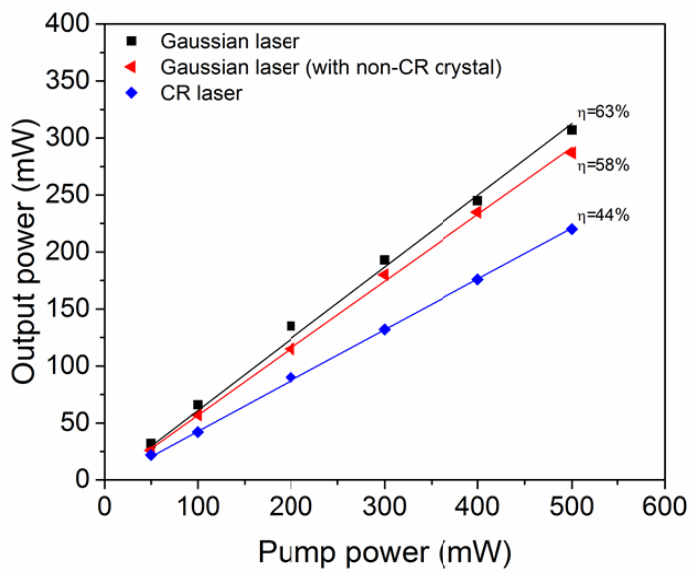

Figure 4. The output power vs. pump power for the free-running Gaussian laser with or without the non-CR crystal as well as for the CR laser.

The formation of the CR beam was also investigated for different degree of focusing of the laser mode into the CRE. It is well-known that the intensity distribution of passive CR beam pattern is affected by the ratio of the CR ring and the input beam radii $\rho_0 = R_0/\omega_0$. A clear CR beam pattern can be formed for $\rho_0 >> 1$ [8]. This could be done in our experiments by using the R3 mirrors with different radius of curvature (ROC) so that the laser mode size focused into the CRE could be controlled. For ROC = −100 mm the CR beam with thinner Poggendorff ring could be generated (see figure 5 (a)). By increasing the ROC of the R3 mirror, the CR ring pattern became thicker. For ROC = −300 mm the inner ring of the CR patter collapsed into a central spot and for a larger ROC = −750 mm the CR beam exhibited a crescent-like pattern, similar to the previously demonstrated CR lasers [10,12–14].

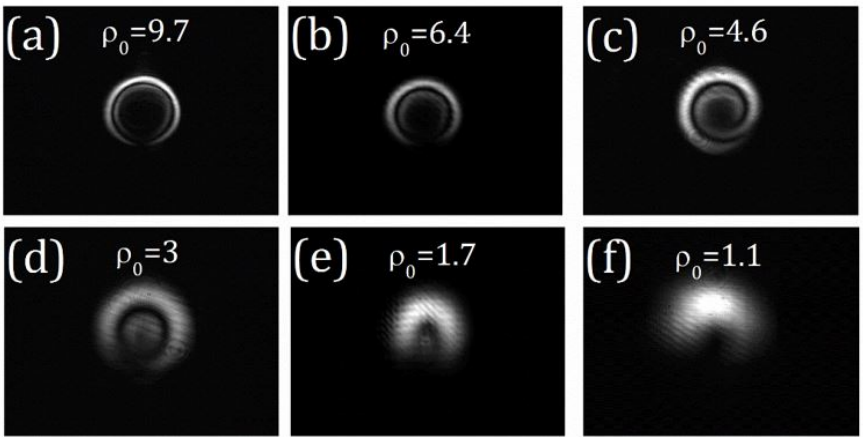

Figure 5. The CR laser beam patterns for different ROCs of the focusing mirror R3. (a) R3 = −100 mm, (b) R3 = −150 mm, (c) R3 = −200 mm, (d) R3 = −300 mm, (e) R3 = −500 mm, (f) R3 = −750 mm. The numbers show the estimated ratio ρ_0 of the CR ring radius (R_0) to the Gaussian mode waist radius (in our case R_0 = 306 μm). For all cases the position of the image plane was similar.

In order to investigate the laser mode evolution in the CR Nd:YVO_4 laser cavity, the laser mode leakage from the HR mirror (i.e. opposite arm of the cavity) was also imaged and compared to the equivalent laser mode in the typical (i.e. Gaussian mode) regime of operation (see figure 6). As can be seen, the laser mode in the CR regime exhibited similar distribution to the far-field CR beam (i.e. Raman spot) with concentric intensity background, which was absent in case of the Gaussian laser mode. Therefore, different spatial profile of the resonating modes in the CR and Gaussian lasers could cause the reduction in laser output power in CR regime (see figure 4) since the overlap between the pump beam and the laser mode in the Nd:YVO_4 crystal was affected [34].

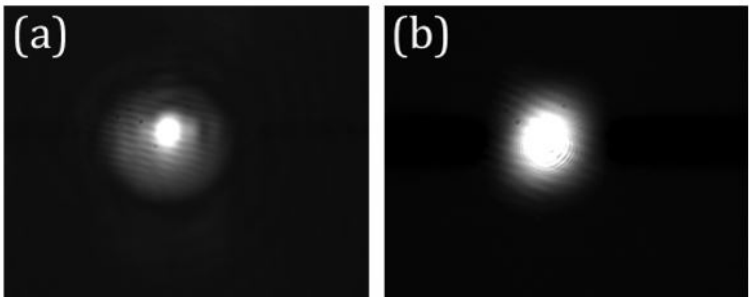

Figure 6. Intensity profiles of the laser output beams from the HR arms for the (a) CR and (b) Gaussian lasers.

4. CONCLUSIONS

In summary, a CR laser with separate laser and intracavity CR media was demonstrated. The separation of the laser gain medium and the CRE in the laser cavity made it possible to conveniently transform a laser with Gaussian output beam into a CR laser beam with well-characterized CR ring pattern. By using an a-cut Nd:YVO_4 crystal as the laser medium and a KGW crystal with cut along its optical axis as the CRE, the laser generated a well-resolved CR beam with maximum output power of 220 mW for pump power of 500 mW. It was also shown that the focusing condition of the laser mode on the CRE considerably affected the CR beam pattern and for a tighter focusing of the laser mode into the CRE, a thinner Poggendorff ring could be generated. In addition, it was shown that the laser mode in the CR regime exhibited different transformation by observing the laser mode leakage from the opposite cavity arm. This could be responsible for the reduction of the laser output power in the CR regime when compared with the Gaussian beam laser. In general, the demonstrated CR laser has the potential of power scaling and more flexible design parameters (e.g. wavelength or gain medium) [35-41] due to the separation of the laser medium and the CRE. Extension to the efficient diode-pumped Yb-ion lasers is particularly interesting although this will require taking into account re-absorption losses in the gain medium [42]. We believe that the results of this work can be used to further develop the theoretical work and experiments on active CR lasers.

ACKNOWLEDGEMENTS

The authors would like to acknowledge funding of this project provided by the Natural Sciences and Engineering Research Council of Canada (NSERC); University of Manitoba (U of M); E.U.R was partially supported by a Grant of Russian Science Foundation (Grant No. 18-15-00172).

REFERENCES

[1] A. Turpin, Y. V. Loiko, T. K. Kalkandjiev, and J. Mompart, "Conical refraction: fundamentals and applications," Laser Photon. Rev. 10, 750–771 (2016).
[2] A. M. Belsky and A. P. Khapalyuk, "Internal conical refraction of bounded light beams in biaxial crystals," Opt. Spectrosc. 44, 436 (1978).

[3] A. M. Belsky and M. A. Stepanov, "Internal conical refraction of coherent light beams," Opt. Commun. 167, 1–5 (1999).
[4] M. V. Berry, "Conical diffraction asymptotics: fine structure of Poggendorff rings and axial spike," J. Opt. A Pure Appl. Opt. 6, 289–300 (2004).
[5] C. F. Phelan, K. E. Ballantine, P. R. Eastham, J. F. Donegan, and J. G. Lunney, "Conical diffraction of a Gaussian beam with a two crystal cascade," Opt. Express 20, 13201 (2012).
[6] G. S. Sokolovskii, D. J. Carnegie, T. K. Kalkandjiev, and E. U. Rafailov, "Conical Refraction: New observations and a dual cone model," Opt. Express 21, 11125 (2013).
[7] A. Turpin, Y. V. Loiko, T. K. Kalkandkiev, H. Tomizawa, and J. Mompart, "Super-Gaussian conical refraction beam," Opt. Lett. 39, 4349 (2014).
[8] M. V. Berry, M. R. Jeffrey, and J. G. Lunney, "Conical diffraction: observations and theory," Proc. R. Soc. A Math. Phys. Eng. Sci. 462, 1629–1642 (2006).
[9] J. Hellström, H. Henricsson, V. Pasiskevicius, U. Bünting, and D. Haussmann, "Polarization-tunable Yb:KGW laser based on internal conical refraction," Opt. Lett. 32, 2783 (2007).
[10] A. Brenier, "Revealing modes from controlling an off-optical axis conical diffraction laser," Laser Phys. 27, 105001 (2017).
[11] A. Abdolvand, K. G. Wilcox, T. K. Kalkandjiev, and E. U. Rafailov, "Conical refraction Nd:$KGd(WO_4)_2$ laser," Opt. Express 18, 2753 (2010).
[12] A. Brenier, "Lasing with conical diffraction feature in the $KGd(WO_4)_2$:Nd biaxial crystal," Appl. Phys. B 122, 237 (2016).
[13] K. G. Wilcox, A. Abdolvand, T. K. Kalkandjiev, and E. U. Rafailov, "Laser with simultaneous Gaussian and conical refraction outputs," Appl. Phys. B 99, 619–622 (2010).
[14] R. Cattoor, I. Manek-Hönninger, D. Rytz, L. Canioni, and M. Eichhorn, "Laser action along and near the optic axis of a holmium-doped $KY(WO_4)_2$ crystal," Opt. Lett. 39, 6407 (2014).
[15] Y. Sato, T. Taira, N. Pavel, and V. Lupei, "Laser operation with near quantum-defect slope efficiency in Nd:YVO_4 under direct pumping into the emitting level," Appl. Phys. Lett. 82, 844–846 (2003).
[16] M. Nadimi, T. Waritanant, and A. Major, "High power and beam quality continuous-wave Nd:$GdVO_4$ laser in-band diode-pumped at 912 nm," Photonics Res. 5, 346 (2017).
[17] T. Waritanant and A. Major, "Thermal lensing in Nd:YVO_4 laser with in-band pumping at 914 nm," Appl. Phys. B 122, 135 (2016).
[18] T. Waritanant and A. Major, "High efficiency passively mode-locked Nd:YVO_4 laser with direct in-band pumping at 914 nm," Opt. Express 24, 12851 (2016).
[19] M. Nadimi, T. Waritanant, and A. Major, "Passively mode-locked high power Nd:$GdVO_4$ laser with direct in-band pumping at 912 nm," Laser Phys. Lett. 15, 15001 (2018).
[20] T. K. Kalkandjiev and M. A. Bursukova, "Conical refraction: an experimental introduction," Proc. SPIE 6994, Photon Management III, 69940B (2008).
[21] D. P. O'Dwyer, K. E. Ballantine, C. F. Phelan, J. G. Lunney, and J. F. Donegan, "Optical trapping using cascade conical refraction of light," Opt. Express 20, 21119–21125 (2012).
[22] C. McDonald, C. McDougall, E. Rafailov, and D. McGloin, "Characterising conical refraction optical tweezers," Opt. Lett. 39, 6691-6694 (2014).
[23] A. Turpin, Y. Loiko, T. K. Kalkandjiev, and J. Mompart, "Free-space optical polarization demultiplexing and multiplexing by means of conical refraction," Opt. Lett. 37, 4197 (2012).
[24] I. V. Mochalov, "Laser and nonlinear properties of the potassium gadolinium tungstate laser crystal $KGd(WO_4)_2:Nd^{3+}$-(KGW:Nd)," Opt. Eng. 36, 1660 (1997).
[25] P. Loiko, S. Manjooran, K. Yumashev, and A. Major, "Polarization anisotropy of thermal lens in Yb:$KY(WO_4)_2$ laser crystal under high-power diode pumping," Appl. Opt. 56, 2937–2945 (2017).
[26] R. C. Talukder, M. Z. E. Halim, T. Waritanant, and A. Major, "Multiwatt continuous wave Nd:KGW laser with hot-band diode pumping," Opt. Lett. 41, 3810 (2016).
[27] M. Z. E. Halim, R. C. Talukder, T. Waritanant, and A. Major, "Passive mode locking of a Nd:KGW laser with hot-band diode pumping," Laser Phys. Lett. 13, 105003 (2016).
[28] R. Akbari, K. A. Fedorova, E. U. Rafailov, and A. Major, "Diode-pumped ultrafast Yb:KGW laser with 56 fs pulses and multi-100 kW peak power based on SESAM and Kerr-lens mode locking," Appl. Phys. B 123, 123 (2017).

[29] R. Akbari and A. Major, "High-power diode-pumped Kerr-lens mode-locked bulk Yb:KGW laser," Appl. Opt. 56, 8838–8844 (2017).
[30] A. Major, R. Cisek and V. Barzda, "Development of diode-pumped high average power continuous-wave and ultrashort pulse Yb:KGW lasers for nonlinear microscopy," Proc. SPIE 6108, 61080Y (2006).
[31] R. Akbari, H. Zhao, and A. Major, "High-power continuous-wave dual-wavelength operation of a diode-pumped Yb:KGW laser," Opt. Lett. 41(7), 1601-1604 (2016).
[32] H. Zhao, A. Major, "Orthogonally polarized dual-wavelength Yb:KGW laser induced by thermal lensing," Appl. Phys. B 122(6), 163-169 (2016).
[33] H. Zhao, A. Major, "A continuous wave Yb:KGW laser with polarization-independent pump absorption," Laser Phys. 23, 095001 (2013).
[34] Y. V. Loiko, G. S. Sokolovskii, D. Carnegie, A. Turpin, J. Mompart, and E. U. Rafailov, "Laser beams with conical refraction patterns," Proc. SPIE 8960, p. 89601Q (2014).
[35] T. Waritanant, A. Major, "Discretely selectable multiwavelength operation of a semiconductor saturable absorber mirror mode-locked Nd:YVO_4 laser," Opt. Lett. 42, 3331-3334 (2017).
[36] M. Nadimi, T. Waritanant, A. Major, "Discrete multi-wavelength tuning of a continuous wave diode-pumped Nd:$GdVO_4$ laser," Laser Phys. Lett. 15(5), 055002 (2018).
[37] M. Nadimi, A. Major, "Continuous-wave dual-wavelength operation of a diode-pumped Nd:$GdVO_4$ Laser at the 1063 & 1071 nm, 1063 & 1083 nm and 1083 &1086 nm wavelength pairs," Laser Phys. 28(9), 095001 (2018).
[38] T. Waritanant, A. Major, "Dual-wavelength operation of a diode-pumped Nd:YVO_4 laser at the 1064.1 & 1073.1 nm and 1064.1 & 1085.3 nm wavelength pairs," Appl. Phys. B 124(5), 87 (2018)
[39] S. Ghanbari and A. Major, "High power continuous-wave dual-wavelength alexandrite laser," Laser Phys. Lett. 14(10), 105001 (2017).
[40] S. Ghanbari and A. Major, "High power continuous wave Alexandrite laser with green pump," Laser Phys. 26(7), 75001 (2016).
[41] S. Manjooran, P. Loiko, A. Major, "A discretely tunable dual-wavelength multi-watt Yb:CALGO laser," Appl. Phys. B 124(1), 13 (2018).
[42] H. Zhao, A. Major, "Dynamic characterization of intracavity losses in broadband quasi-three-level lasers," Opt. Express 22, 26651-26658 (2014).